© Universiti Tun Hussein Onn Malaysia Publisher's Office

IJIE

http://penerbit.uthm.edu.my/ojs/index.php/ijie
ISSN : 2229-838X e-ISSN : 2600-7916

The International Journal of Integrated Engineering

Flow Analysis of Intake Manifold Using Computational Fluid Dynamics

Syafiqah Ruqaiyah Saiful Azam[1], Shaiful Fadzil Zainal Abidin[1], Izuan Amin Ishak[1], Amir Khalid[1], Norrizal Mustaffa[1], Ishkrizat Taib[2], Safra Liyana Sukiman[3], Nofrizalidris Darlis[1*]

[1]Faculty of Engineering Technology,
University Tun Hussein Onn Malaysia (UTHM), Pagoh Education Hub, Pagoh, Muar, Johor, MALAYSIA

[2]Faculty of Mechanical and Manufacturing Engineering,
University Tun Hussein Onn Malaysia (UTHM), Batu Pahat, MALAYSIA

[3]Centre for Language Studies,
University Tun Hussein Onn Malaysia (UTHM), Batu Pahat, MALAYSIA

*Corresponding Author

DOI: https://doi.org/10.30880/ijie.2023.15.01.008
Received 16 June 2021; Accepted 14 November 2021; Available online 28 February 2023

Abstract: The main element of the air intake system is an intake manifold. These are the main components which control the flow value that will be used in the combustion chamber. This study aims to analyse the velocity of flow distribution in all runners and to compare the design of intake manifold in previous study. Simulations are performed on two types of intake manifold design which are Design 1, the inlet end is located next to the regulator chamber whilst for Design 2, the inlet end is in the middle of regulator chamber. Intake manifold parameters such as velocity distribution, unevenness and pressure losses along the runner are used to determine the better design for better performance. From the results, the velocity, and the pressure of intake manifold of these two types of design are determined. Compared with previous study, the velocity difference is 0.05%. This showed that the simulation result obtained in this study is in accordance with previous study. Next, the percentage difference between Design 1 and previous design is approximately 4%. Furthermore, the pressure losses between Design 1 and Design 2 are 0.3% and Design 1 achieved the range of acceptable values between 2500Pa to 3000Pa. The results of the velocity distribution, the evenness of each runner and the value of pressure losses shows that Design 1 met all the criteria and exhibited the best design improvement as compared to the previous design with 2% improvement.

Keywords: Intake manifold, internal flow, pressure losses, Computational Fluid Dynamics (CFD)

1. Introduction

The intake manifold is the most critical part of an engine for better performance. A set of tubes located at the top of the engine supply fresh air to the cylinders. It collaborates with the air intake, throttle body, and fuel delivery system to ensure that the engine burns the correct combination of air and fuel. The intake manifold functions by directing air via the intake and throttle body into the intake manifold's plenum. This plenum evenly distributes air into each runner. During the intake stroke, the piston descends, creating low pressure in the cylinder. This sucks air into the cylinder from the runner (a high-pressure area). When the inlet valve closed, pressure waves create, which restore the air to the cylinder. When the intake valve returns to its original position, it bounces off the intake and returns into the cylinder. This is done for each cylinder until the engine is switched off [1]. The intake manifold guarantees that enough air is supplied when the valve opens for each intake stroke and that all cylinders receive the same amount of air.

*Corresponding author: nofrizal@uthm.edu.my

Today, the most popular intake manifold innovation is constructing the intake manifold, the runner's inlet, the runner's exit, and the velocity of the fluids entering each cylinder of the runner. Jianmin Xu [2] studied the design of intake manifold utilizing the 3 different models of different inlet end had proposed the best design by analyzing the parameters used such as velocity distribution and pressure drops of the system [2]. In addition, a study of the intake manifold angle has shown that the high intake manifold angle will improve airflow within the intake manifold. This is because the bending manifold causes lower air resistance [3]. Besides that, Ch. Indira Priyadarshini asserted that the intake manifold can be done through numerical simulation rather than running an experiment that incurred cost and timing [4]. CFD programs using turbulence models of k-ε, SST, RMS, and others were developed to accurately predict velocities [5].

Numerous researchers studied the velocity distribution in the runner's intake to get an even distribution of each cylinder for better performance. This study develops three-dimensional (3D) models for the engine employing two design of new intake manifolds. The study presents the basic optimization design of the intake manifold to accomplish velocity distributions in all runners and compares it to the previous study's intake manifold design.

2. Methodology

2.1 Simplified Geometry Model of Intake Manifold

Figure 1 illustrates three-dimensional models of two intake systems used in this investigation. An inlet end, regulator chamber, and intake manifold runner comprise the intake system. There are two types of intake manifold structures proposed. Design 1's inlet ends are positioned close to the regulator, whereas Design 2's inlet ends are in the center of the regulator chamber. Later, Jianmin Xu [2] found that the model is likewise positioned in the center and side of the regulator. Hence, a simpler model is simulated to study the intake manifold performance using different locations of inlet end.

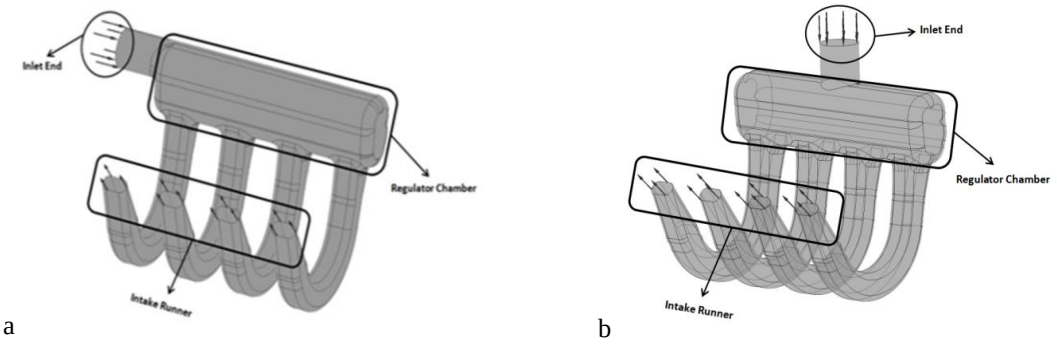

Fig. 1 - Geometry models of design intake manifold (a) design 1; (b) design 2

2.2 Computational Fluid Dynamics (CFD)

A computational domain of simplified intake manifold with two types of intake manifold are drawn using SolidWorks 2018. The software is used to build a solver, which is made up of mathematical algorithms that simulate and analyse airflow [14]. To compute fluid flow parameters, the inlet end's front surface is set to normal speed in the inlet boundary, while the face outlet of each manifold is set to pressure outlet boundary and others to the wall boundary. Shear Stress Transport (SST), a typical turbulence model, is used [16-17]. These models are imported into ANSYS CFX19.2 for finite volume discretization of the Navier-Stroke equation [18]. Each computational domain model is formed into a tetrahedral mesh [13], as seen in Figure 2. Due to the intricacy of the intake manifold, the tetrahedral mesh is examined, and it is essential to achieve two-point nodes between the fluid domain and the wall domain [10]. The velocity input and pressure exit are computed to solve the continuity and Navier-Stokes equations. The Navier-Stroke equations are defined as shown in Eq. (2) [7] under the assumptions of continuity, non-slip wall, and 0 Pa static pressure.

$$\rho \frac{\partial u}{\partial t} + \rho(u \cdot \nabla)u = -\nabla P + \mu \nabla^2 u \quad (1)$$

Where u is the primary vector u= [u, v, w] and P is the pressure that vary in space x, y, z and T is time.

2.3 Analysis of Calculation Results

Determining the flow of intake manifold coefficients of each outlet is the common approach of analyzing intake

uniformity. The largest unevenness, E, denotes uneven engine intake. The formula as follows:

$$\mathbf{E} = (\mathbf{Q}\text{max} - \mathbf{Q}\text{min}) / \mathbf{Q}\text{me} \quad (2)$$

Where E is maximum unevenness, Qmax is the maximum flow rate of export quality, Qmin is the minimum flow rate of export quality and Qme is the average mass flow rate.

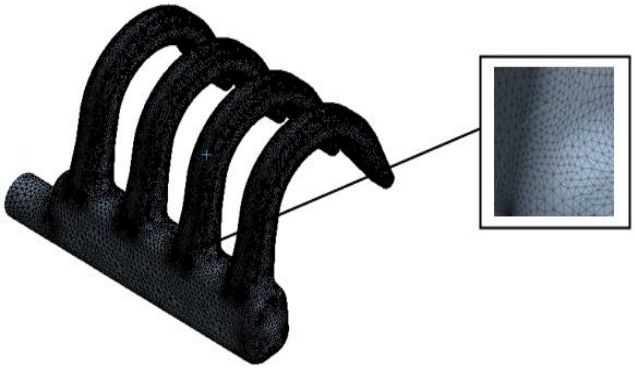

Fig. 2 - Mesh computational domain

3. Results

3.1 Grid Independence Test

Grid Independence Test (GIT) is an expression that defines the optimum numerical accuracy estimates of computed outcomes based on numerical elements [6,7,12]. The inlet end, the regulator chamber, and the intake runner are all covered by this computational domain for numerical calculation. The cell size ranges from coarse to ultra, and the element count ranges between 120k and 250k. Figure 2 depicts the velocity distributions of Design 1 intake manifolds, whereas Figure 3 depicts the velocity distributions of Design 2. According to these two figures, the velocity distribution of 150k nodes to 250k nodes is not significantly affected with the average relative error of 1%. The mesh size is gradually increased until the improvement in mesh size no longer increases significantly in performance [15]. The following simulations are set at around 150k nodes or higher. Since these models achieve grid independence tests, cell sizes should be reduced successively so errors are minimized due to discretization.

3.2 Validation of Numerical Result in Previous Study

Figure 3 shows that the validation of the numerical simulation result of a two-line graph representing the previous and present study. Validation of the CFD simulation findings is accomplished by comparing the current study with the prior research by changing the parameter of the inlet end velocity from 11m/s to 18m/s for the first runner and generating a line graph. The trends of velocity line graph simulation in the present study show that the velocity outlet gradually increased as the inlet velocity increased. This line graph is quite like the previous pattern. The different pattern for these lines graphs is seen to be reasonable as the consistency the flow velocity outlet increases with approximately around 0.04 percent difference in the present and previous study.

3.3 Velocity Distributions

Figures 6(a) and 6(b) show velocity contour plots of airflow from the intake runner's inlet to output. Figure 6(a) shows the intake end near to the regulator chamber, whereas Figure 6(b) shows the inlet in the middle of the regulator chamber. The maximum airflow velocity shows on the contour is around 33m/s whilst the minimum flow velocity shows around 4m/s for both designs. It is notable in the left sides of the legend value in which the values of maximum and minimum can be observed.

Next, by observing the result of the velocity contour plot in Figure 6(a), the color of red clearer can be seen on the contour for the first intake runner when it is open. It is followed by the second runner opening in which the red contour becomes darker, and so on until the fourth runner. This demonstrates that the airflow velocity of the manifold is great distant from the intake end and modest near the entry end, which is consistent with the notion outlined in the prior research [2,8]. This might be due to length of chamber. By increasing its length, airflow resistance to travel also increases and the velocity output or the performance will be reduced.

When the first intake runner for Design 2in Figure 6(b) is opened, it is evident that the red velocity contour is dimmer than Design 1. The same persists in the second runner for Design 2 in which the red contour looks dimmer when it is compared to Design 1, which shows that the flow velocity for Design 1 is better than Design 2.

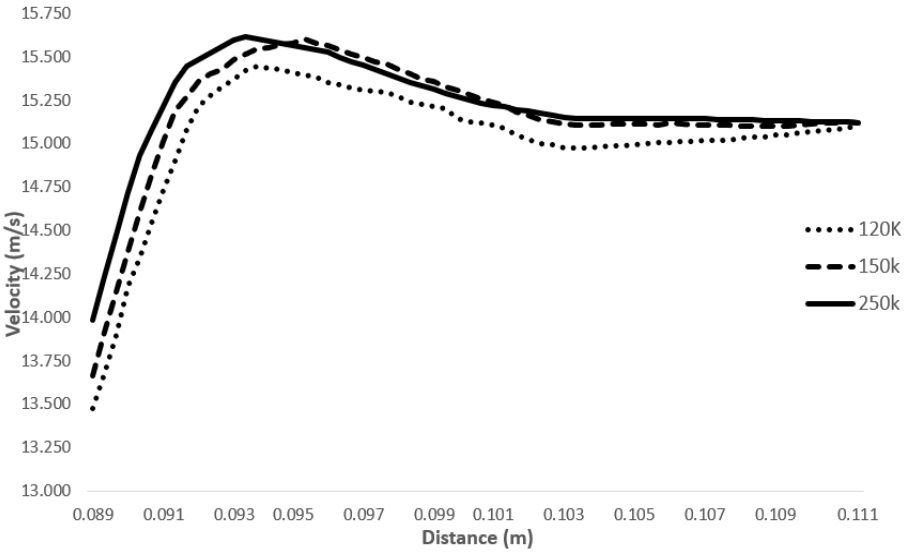

a

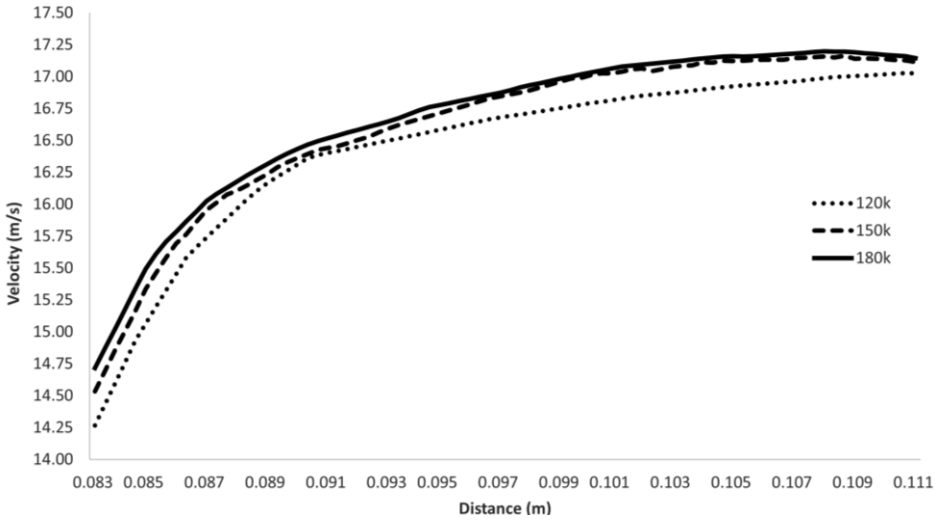

b

Fig. 4 - Grid independence test for (a) design 1; (b) design 2

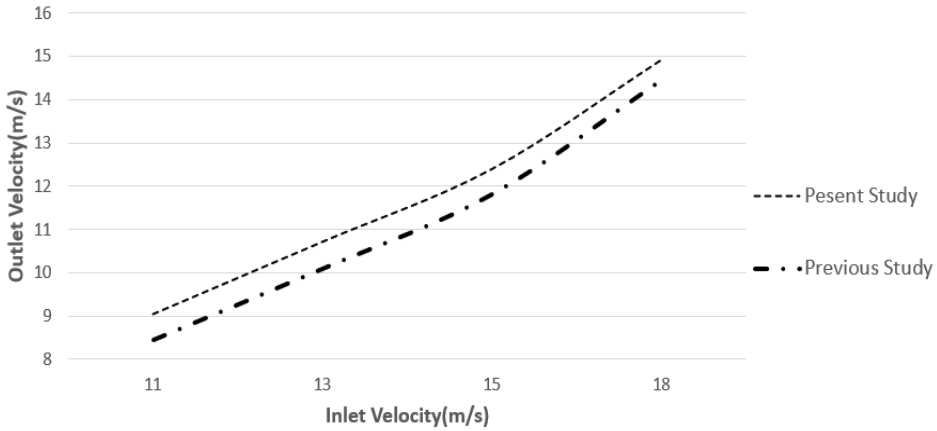

Fig. 3 - Comparison of numerical results of present and previous study for intake runner 1

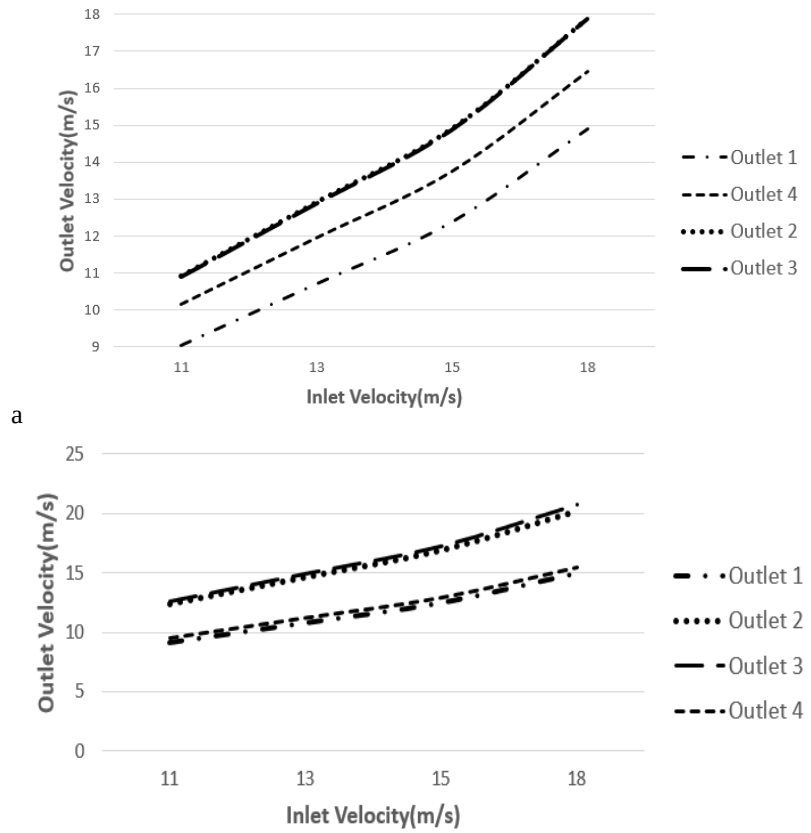

Fig. 5 - Velocity at outlet with variable inlet velocities for (a) design 1; (b) design 2

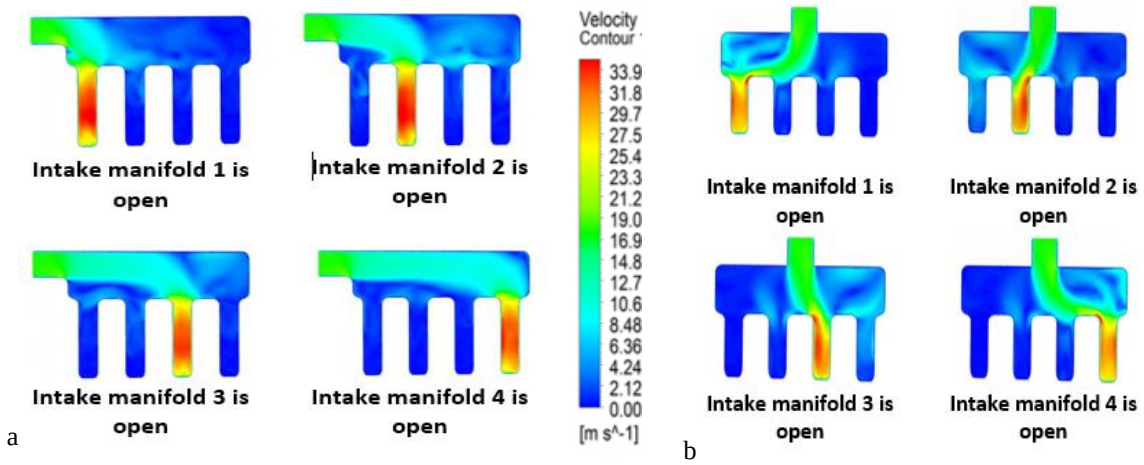

Fig. 6 - The velocity contour of intake manifold for (a) design 1; (b) design 2

3.4 Determined The Vortex Phenomenon and Unevenness of the Design

Figure 7 shows the velocity vector of the intake manifold for Design 1 and Design 2. Figures 7(a) and 7(b) show more eddies in the first runner and fourth runner for Design 1 while in Design 2, it occurred in the second and the third runner. This phenomenon, namely the vortex phenomenon, can cause the increase of flow resistance. As the resistance flow increases, the intake amount of airflow entering the intake runner will reduce and affect the combustion process and the engine's performance.

The evenness of airflow distribution is also one of the factors that determine better engine performance. Based on simulation results, the unevenness, E of the calculated inlet end located at the side (Design 1) is 0.3percent, contradict with previous research annotated by Jianmin Xu [2] (4.72 percent). The percentage difference between Design 1 and previous research is approximately 4 percent thus, this signifies that the airflow evenness of intake manifold Design 1 is

better and reasonable. If the airflow in all runners is distributed evenly, the process of combustion in combustion chamber will occur simultaneously hence, producing more power output for the engine.

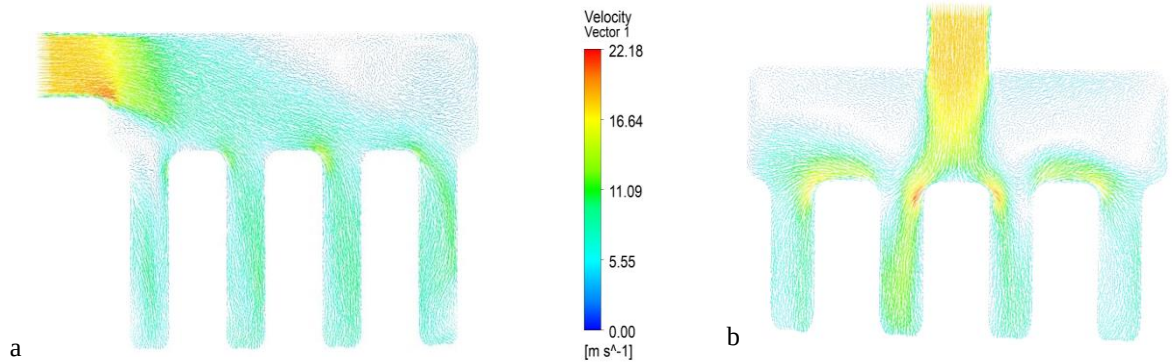

Fig. 7 - The velocity vector contour of intake manifold for (a) design 1; (b) design 2

3.5 Pressure Losses

Another factor that affects engine performance is pressure losses [11]. A previous study reported that the pressure losses between 2500Pa to 3000Pa were the best choice, and the decreasing of velocity will result more pressure losses in the intake runner [8]. As a result, pressure losses less than 3000Pa are chosen as a reference in this study. Figure 8 depicts a comparison of pressure losses for Designs 1 and 2. As seen in Figure 8, Design 1 had a consistent pattern for all intake runners, but Design 2 had instability and higher-pressure losses. This is owing to the varied geometric design employed in each design. In Design 1, the intake end is positioned close to the regulator chamber, but in Design 2, the inlet end is in the center of the regulator chamber. P. Ragupathi et al. previously discovered that the ideal design inlet end situated in the middle of a regulator produced less pressure losses compared to the the inlet end located near to the side regulator [8].

In this present study, the result contradicts with the previous study in which the inlet end located next to the side regulator is better than in the middle. These contrary results might be due to the geometry of Design 2 that did not meet its geometrical specifications as in the previous study. However, its physical design looks identical. In summary, the intake runner of Design 1 did not exceed the preference value of 2500Pa to 3000Pa. This shows that the geometry design of Design 1 is feasible as there is evidence of different pressure drop between each runner with approximately less than one percent. Table 1 shows the pressure losses of individual runners predicted between the inlet and the outlet points of related runners at the mass flow rate of 0.0416kg/s for Design 1 while 0.04144ks/s. The predicted pressure loss for each runner is compared and the results are summarized in the following table (Table 1) both designs.

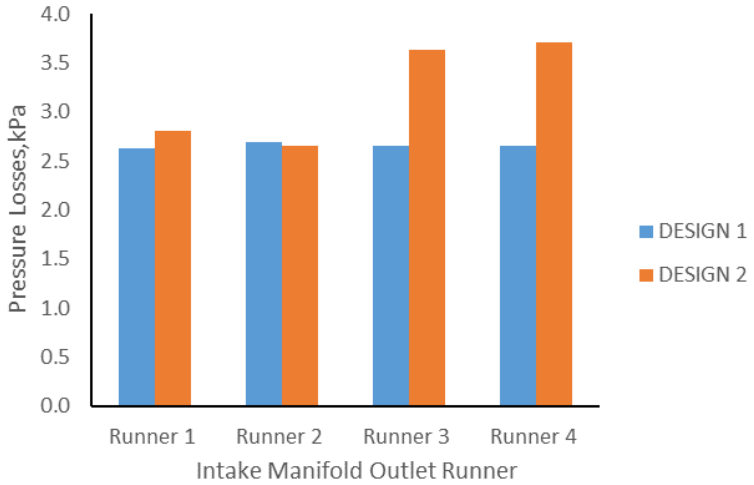

Fig. 8 - The pressure losses between 2 designs

Figure 9 shows the result of velocity outlet design 1 and previous research. The results indicate that the new designed intake manifold (design1) performs better than the previous design as the velocity measured from the outlets improved by 2%. The engine's output increases when the velocity outlet increases, since the amount of air entering the

intake manifold increases. Increasing air entering the combustion chamber through the new intake manifold design results in better and improved combustion efficiency. As a result, the engine performance and efficiency will be improved.

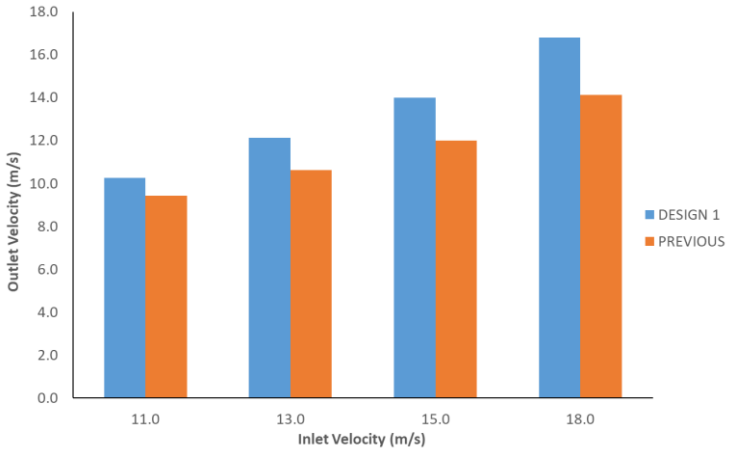

Fig. 9 - Result of velocity outlet for design 1 and previous design

4. Conclusions

Finally, CFD simulation of two types of intake manifolds is performed, and the flow field of the model is examined. This study compares the intake manifold Designs 1 and 2 from earlier studies. The findings suggest that the inlet end positioned near to the regulator can significantly increase intake uniformity while also improving an engine's intake efficiency and combustion quality. The data also reveal that Design 1 is superior for performance since it has a smaller percentage of estimated unevenness, E, and fewer pressure losses than Design 2, which has its intake end in the center of the regulator. The numerical simulation of the intake manifold system is performed using computational fluid dynamic theory to produce a feasible and effective way of analysis. The research also explains its conclusions, which the pressure losses and flow of the intake manifold are two significant assessment indicators, and that Design 1 fulfils these two-design parameters.

Acknowledgement

This research is supported by Ministry of Education (MOE) through Fundamental Research Grant Scheme (FRGS/1/2020/TK02/UTHM/03/4). The author would like to thank Faculty of Engineering Technology, Universiti Tun Hussein Onn Malaysia for providing feasible research facilities for this study.

References

[1] Andersson, B. (2011). Computational fluid dynamics for engineers. Cambridge University Press.
[2] Hamid, M. F., Idroas, M. Y., Sa'ad, S., Heng, T. Y., Mat, S. C., Alauddin, Z. A. Z., Shamsuddin, K. A., Shuib, R. K., & Abdullah, M. K. (2020). Numerical investigation of fluid flow and in-cylinder air flow characteristics for higher viscosity fuel applications. Processes, 8(4). https://doi.org/10.3390/PR8040439
[3] Holkar, R., N, Y., & Sule-Patil. (2017). Kesejahteraan Subjektif Warga Emas di Institusi Penjagaan Awam. Numerical Simulation of Steady Flow through Engine Intake System Using CFD, 12(1), 30–45. https://doi.org/10.9790/1684-12123045
[4] Hushim, M. F., Alimin, A. J., Razali, M. A., Mohammed, A. N., Sapit, A., & Carvajal, J. C. M. (2016). Air flow behaviour on different intake manifold angles for small 4-stroke PFI retrofit KIT system. ARPN Journal of Engineering and Applied Sciences, 11(12), 7565–7571.
[5] Ponnusamy, R., Ragupathi, P., Rajkumar, S., & Hussain, R. S. (2018). DESIGN AND ANALYSIS OF DIESEL ENGINE INTAKE MANIFOLD USING CFD SIMULATION. www.ijmtes.com
[6] Priyadarsini, I. (2016). Flow Analysis of Intake Manifold using Computational Fluid Dynamics. International Journal of Engineering and Advanced Research Technology, 2(1), 1–5. www.ijeart.com
[7] Seman, C. M. H. M. C., Marzuki, N. A., Darlis, N., Marsi, N., Salleh, Z. M., Ishak, I. A., Taib, I., & Sukiman, S. L. (2020). Comparison of hemodynamic performances between commercially available stents design on stenosed femoropopliteal artery. CFD Letters, 12(7), 17–25. https://doi.org/10.37934/cfdl.12.7.1725
[8] Thundil, R., Raj, K., & Manimaran, R. (2012). Effect of Swirl in a Constant Speed DI Diesel Engine using Computational Fluid Dynamics. In Karuppa & Manimaran CFD Letters (Vol. 4, Issue 4). www.cfdl.issres.net

[9] Xu, J. (2017). Flow analysis of engine intake manifold based on computational fluid dynamics. Journal of Physics: Conference Series, 916(1), 0–8. https://doi.org/10.1088/1742-6596/916/1/012043
[10] Pratap, A. (n.d.). *Intake Manifold Design using Computational Fluid Dynamics M.Tech Dissertation-II*.
[11] Porter, M. A. (n.d.). *Intake Manifold Design using Computational Fluid Dynamics*.
[12] Hamisu, M. T., Jamil, M. M., Sanusi Umar, U., & Sa'ad, A. (2019). CFD Letters Numerical Study Of Flow In Asymmetric 2D Plane Diffusers With Different Inlet Channel Lengths. *CFD Letters*, *11*, 1–21.
[13] Sadah Muhssen, H., Masuri, S. U., Sahari, B., & Hairuddin, A. A. (2019). CFD Letters Computational Fluid Dynamics Investigation of Air-Gas Pre Mixing Controller Mixer Designed for CNG-Diesel Dual-Fuel Engines. *CFD Letters*, *11*, 47–62.
[14] Gurunathan, B. A., Khairuddin, U., Shah, N. N. A., & Martinez-Botas, R. (2020). Influence of double entry volute on incidence angle variation under steady flow: Numerical investigation. *CFD Letters*, *12*(10), 75–89. https://doi.org/10.37934/cfdl.12.10.7589
[15] Almohammadi, K. M., D. B. Ingham, L. Ma, and M. Pourkashan. "Computational fluid dynamics (CFD) mesh independency techniques for a straight blade vertical axis wind turbine."Energy58 (2013): 483-493.
[16] Menter, F. L. O. R. I. A. N. R. "Zonal two equation kw turbulence models for aerodynamic flows." In 23rd fluid dynamics, plasmadynamics, and lasers conference, p. 2906. 1993.
[17] D. Adanta and A. Indra Siswantara, "Assessment of Turbulence Modelling for Numerical Simulations into Pico Hydro Turbine," *Journal of Advanced Research in Fluid Mechanics and Thermal Sciences Journal homepage*, vol. 46, pp. 21–31, 2018.
[18] A. Tariq *et al.*, "Study of Heat Transfer Attributes of Custom Fins for Crank-Rocker Engine Block using ANSYS," *Journal of Advanced Research in Fluid Mechanics and Thermal Sciences Journal homepage*, vol. 62, pp. 235–243, 2019.